

# Liquid-liquid phase transitions in supercooled water studied by computer simulations of various water models

Ivan Brovchenko,<sup>Y</sup> Alfons Geiger,<sup>Y</sup> and Alla Oleinikova<sup>Z</sup>  
 Physical Chemistry, Dortmund University, 44221 Dortmund, Germany  
 (Dated: August 31, 2019)

Liquid-liquid and liquid-vapor coexistence regions of various water models were determined by MC simulations of the isotherms of density fluctuation restricted systems in the NPT ensemble and by MC simulations in the Gibbs ensemble. All studied water models show multiple liquid-liquid phase transitions in the supercooled region: two transitions of the TIP4P, TIP5P and SPCE models and three transitions of the ST2 model. The location of these phase transitions with respect to the liquid-vapor coexistence curve and the glass temperature is highly sensitive to the water model and its implementation. We suggest, that the thermodynamic singularity of real liquid water in the supercooled region at about 228 K is caused by an approach to the spinodal of the first (lowest density) liquid-liquid phase transition. The anomalous behavior of the liquid water density (maximum at 277 K) is related to the second liquid-liquid phase transition, located at positive pressures with a critical point close to the liquid density maximum. A possible order parameter and the universality class of the liquid-liquid phase transitions in one-component fluids is discussed.

## I. INTRODUCTION

Some one-component substances show several amorphous states at low temperatures. This suggests the possible existence of phase transitions between them. Evidence for such phase transitions in supercooled water was obtained both from experiments [1, 2, 3, 4] and simulations [5, 6, 7, 8, 9, 10, 11, 12] (see also Refs. [13, 14, 15] for recent reviews). The presence of phase transitions between different liquid (glassy) states of an isotropic

liquid in the supercooled state (below the freezing temperature) may noticeably influence the properties of a liquid above its freezing temperature. In particular, anomalous, singularity-like behavior of some thermodynamic properties at low temperatures is observed in some fluids [16], including water [17, 18]. Such behavior can be explained by the influence of a distant liquid-liquid phase transition with a critical point located in the supercooled region [5].

Liquid-liquid phase transitions of a one-component liquid may occur in a thermodynamic region where one or both liquid phases are metastable (unstable) with respect to crystallization or evaporation. This makes experimental studies of such phase transitions difficult or even impossible. Fortunately, this is not the case for computer simulations, which can be used to study fluids in metastable or even unstable states. In principle, the coexistence of two liquid phases with an explicit interface between them could be obtained by direct simulations in the NVT ensemble. However, this demands the use of large systems, which can not be equilibrated at low temperatures during reasonable computer simulation times. Decreasing the system size causes a narrowing of the density range, where the coexistence of two phases

with explicit interface can be obtained [19]. In a small enough system, whose size does not exceed some "critical" value, a phase separation with a persistent interface can be prevented completely and a continuous isotherm, joining the two states at subcritical temperatures, can be simulated. The presence of a van der Waals-like loop directly evidences the sub-critical character of an isotherm. This is allowed to detect a liquid-liquid phase transition in ST2 [5, 6, 9, 20, 21, 22] and TIP5P [8] water models. Note, that the unavoidable tendency of the simulated metastable and unstable systems to phase separation ultimately distorts the computed isotherms [23]. Moreover, the "critical" size of the system, which prevents phase separation in the simulation box in the whole density range of the two-phase coexistence, can not be estimated in advance. These factors determine intrinsic shortcomings of the applicability of simulations in the NVT ensemble to study phase transition, which can not be overcome by varying the system size or by improving the sampling. In particular, these shortcomings can lead to the absence of a van der Waals-like loop at sub-critical isotherm close to the critical temperature, resulting in a lower value of the estimated critical temperature of the phase transition.

Simulations in the NPT ensemble can also be used to study low-temperature liquid-liquid phase transitions. An abrupt change of the density along an isobar at some temperature indicates a phase transition. However, it is difficult to distinguish a phase transition from a sharp but continuous change of the density [24, 25]. Only stable and metastable but mechanically unstable states can be explored in the NPT ensemble and, therefore, a continuous isotherm, joining two phase states at subcritical temperatures, can not be obtained. Simulations of subcritical isotherms in the NPT ensemble are accompanied by hysteresis phenomena, which may serve as an indicator of a phase transition. However, the extension of a hysteresis loop depends on the system size and simulation time. As in the case of the NVT ensemble, this

<sup>Y</sup>Electronic address: brov@heineken.chemie.uni-dortmund.de

<sup>Y</sup>Electronic address: alfons.geiger@udo.edu

<sup>Z</sup>Electronic address: alla@heineken.chemie.uni-dortmund.de

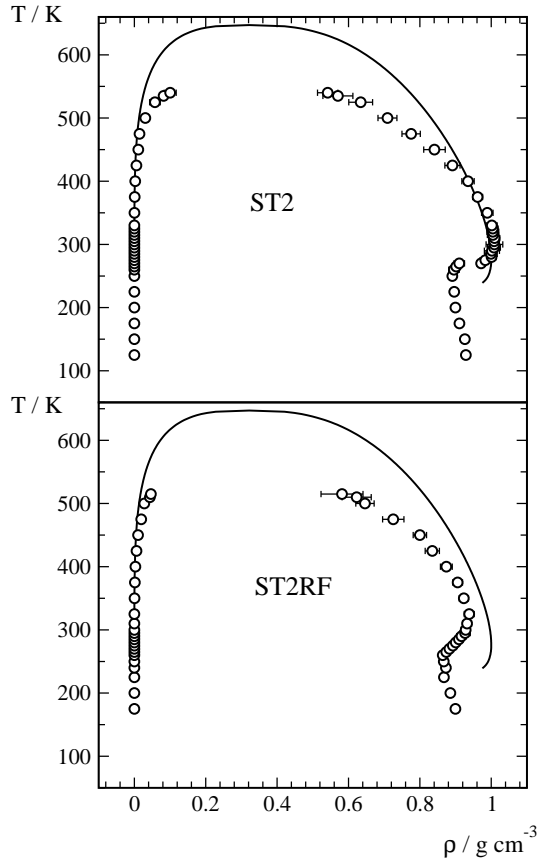


FIG. 1: Liquid-vapor coexistence curve of the ST2 and ST2RF water models (circles). Experimental data [27, 28] are shown by the solid lines.

re ects the fact that extension of such simulations beyond the stable states could be hardly controlled.

The study of phase transitions by simulations in the canonical ensembles can be essentially improved by forcing the system to remain homogeneous even in metastable and unstable states. This can be achieved by restricting the density fluctuations on a mesoscopic scale [23, 26]. Simulations of isotherms in such restricted ensembles enable the location of the liquid-liquid phase transitions at supercooled temperatures [10, 11]. In the present paper we use this method to find liquid-liquid phase transitions of various water models in the supercooled region. In some cases the densities of the coexisting liquid phases were determined directly by simulations in the Gibbs ensemble [10, 11]. To locate liquid-liquid transitions with respect to the liquid-vapor coexistence curve, the latter was simulated in the Gibbs ensemble down to low temperatures. The obtained phase diagrams are used to analyze the sensitivity of the liquid-liquid and liquid-vapor phase transition to the peculiarities of a water model and its implementation. The possible location of the liquid-liquid phase transitions in real water is inferred.

## II. SIMULATION METHODS

ST2 [29], TIP4P [30], TIP5P [31] and SPCE [32] water models were used in our studies. In all cases a simple spherical cutoff  $R_c$  of the intermolecular interactions was used with long-range corrections for the Lennard-Jones potentials (LR LJ corrections). The value of  $R_c$  was 9 Å in all cases, except the TIP4P model, where in the simulations of the liquid-vapor coexistence curve  $R_c$  was 8.5 Å. In accord with the original parameterization of these models [29, 30, 31, 32], no long-range corrections for the Coulombic interaction (LRCI corrections) were included. Additionally, we used the ST2 water model including a reaction field to account for LRCI corrections (ST2RF water model hereafter), which has already been studied intensively in the supercooled region [5, 6, 9, 20, 21, 22]. The liquid-vapor coexistence curve of various water models was obtained by Monte Carlo (MC) simulations in the Gibbs ensemble (GEMC) [33]. The coexistence of different water phases at supercooled temperatures was studied by GEMC simulations and by simulations of isotherms in the density fluctuation restricted NPT ensemble [23, 26].

### A. MC simulations of the liquid-vapor and liquid-liquid coexistence in the Gibbs ensemble

The liquid-vapor coexistence of water was simulated by direct equilibration of the two coexisting phases in the Gibbs ensemble [33]. The total number  $N$  of molecules in the two simulation boxes was about 600, except of the case of the TIP4P model, where  $N$  was about 300 to 400, depending on temperature. The use of efficient techniques for the molecular transfers (see Ref.[34] for more details) allowed to extend the simulated coexistence curves deeply into the supercooled region. Even at extremely low temperatures the number of successful molecular transfers in the course of the simulations always exceeded  $10N$  and achieved  $100N$  at high temperatures. The critical temperature and critical density of the liquid-vapor coexistence curves were estimated by fitting the order parameter with a scaling law including one correction term and by fitting the diameter to a second order polynomial. For this fitting procedure the coexistence curve above the liquid density maximum was used.

The coexistence between liquid water phases of different densities was also studied by GEMC simulations. The extremely low acceptance probability for molecular transfers between two dense liquid phases at low temperatures practically prevents such simulations at temperatures below 260 K and densities above 1.3 g cm<sup>-3</sup>. Another complication is caused by the expected rather small difference between the densities of coexisting liquid phases. GEMC simulations may move toward two coexisting phases, when the average density  $\rho_{av}$  in the two simulation boxes is in the two-phase region. The initial

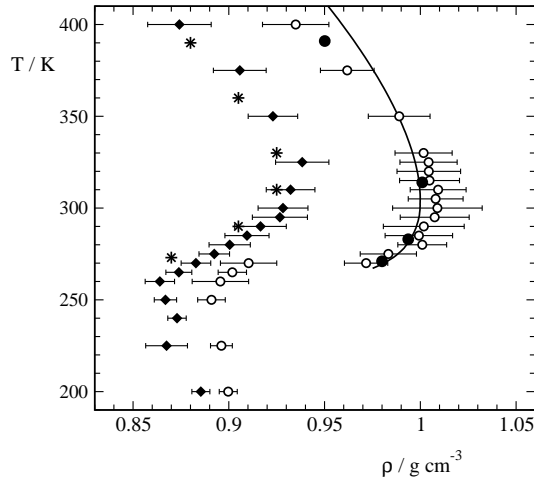


FIG. 2: Liquid densities of ST 2 (open circles) and ST 2RF (solid diamonds) water models along the liquid-vapor coexistence curve. Simulation data at  $P = 0$  for the ST 2 model [29] and the ST 2RF model [6] are shown by solid circles and stars, respectively. Experimental data [27, 28], shifted upwards by 28, are shown by the solid line.

choice of this average density determines the box sizes and numbers of molecules in both boxes, which have to be adequate to reproduce the properties of both coexisting phases. This strongly limits the range of  $\rho_{av}$ , which are appropriate for such studies. Therefore, initially we have equilibrated several configurations of liquid water with different densities in the interval from 0.90 to 1.25 g cm<sup>-3</sup> by MC simulations in the NVT ensemble. Then, several pairs of these configurations with density differences from 0.10 to 0.20 g cm<sup>-3</sup> were used as starting configurations for GEMC simulations. The number of successful molecular transfers was about  $N$  at  $T = 260$  K,  $2N$  at  $T = 270$  K and essentially more at higher temperatures. In such simulations any choice of the average density  $\rho_{av}$  at  $T > 270$  K resulted in comparatively fast (less one month of computer time on a GHz processor) equalization of the densities in the two boxes. The same result was obtained also at  $T = 260$  or 270 K, when  $\rho_{av}$  was about 1.10 g cm<sup>-3</sup>. However, when the average density  $\rho_{av}$  was about 0.95 and 1.05 g cm<sup>-3</sup> the water densities in the two boxes did not tend to equalize at  $T = 260$  and 270 K even during extremely long simulation runs (several months of computer time on a GHz processor) but a stable liquid-liquid equilibrium was reached. It should also be noticed, that we have failed to get the coexistence of two liquid water phases, when starting from two equal densities in the two simulation boxes.

## B. MC simulations in the restricted NPT ensemble

An extension of the isotherm into metastable or unstable regions can be achieved by simulations in the density fluctuation restricted ensemble [23, 26], which allows the

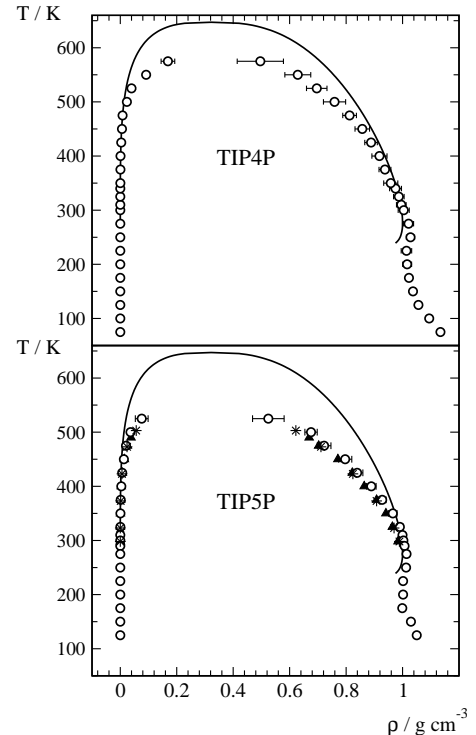


FIG. 3: Liquid-vapor coexistence curve of TIP4P and TIP5P water models (circles). Simulation data of Ref.[35] and Ref.[36] are shown by triangles and stars, respectively. Experimental data [27, 28] are shown by solid lines.

simulation of an artificial single-phase state. The simulation box with  $N$  molecules has to be divided into  $n$  equal subcells. In the general case, the number  $N_i$  of molecules in the  $i$ -th subcell should satisfy the following constraint:

$$N/n \leq N_i \leq N/n + 1; \quad (1)$$

where  $N$  is the maximum allowed deviation of molecules in the subcell from the average value  $N/n$ . Such a constraint can be fulfilled in MC simulations by rejecting those moves, which violate Eq.1. The value  $N/n$  should be small enough to exclude phase separation in each subcell, whereas too small values of  $N/n$  could result in the freezing of the simulated liquid. MC simulations in the restricted NVT ensemble were successfully applied for reproducing the liquid-vapor coexistence curve of LJ uid [23, 26]. In the case of liquid-liquid coexistence in a one-component uid the densities of the coexisting phases could have rather close values (difference < 10%). So, even  $N = 1$  could result in a phase separation in a simulation box with several hundreds molecules. Therefore, we imposed  $N = 0$ , which could noticeably suppress the density fluctuations in the NVT ensemble [23, 26]. Imposing this local restriction in an NPT simulation, the fluctuation of the average density is not restricted. This method can be applied for simulations of stable and metastable, but not for unstable states.

In our implementation of the restricted NPT ensemble, the cubic simulation box with 513 water molecules

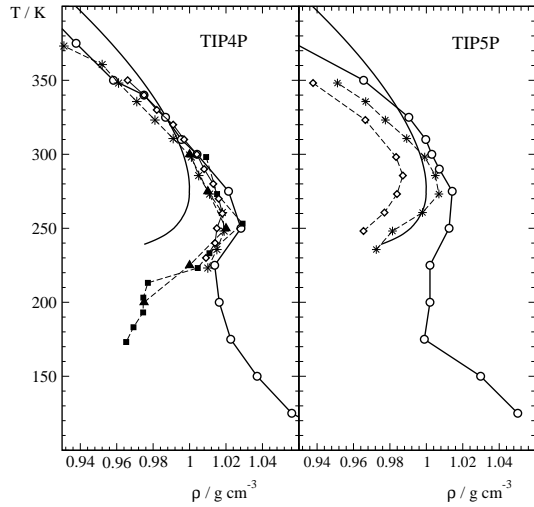


FIG. 4: Liquid densities of TIP4P and TIP5P water models along the liquid-vapor coexistence curve (open circles). Simulation data at  $P = 0$  for the TIP4P model: squares [37], triangles [6], stars [38], diamonds [39]. Simulation data at  $P = 0$  for the TIP5P model: stars [31], diamonds [35]. Experimental data [27, 28] are shown by solid lines.

was divided into 27 equally sized cubic subcells which contain an equal number (19) of molecules. The number of molecules in each subcell was kept unchanged in the course of the MC simulations. Typically up to  $2 \times 10^5$  molecular moves per molecule were done in the course of a MC simulation run. Several isotherms between 150 and 300 K were simulated for each studied water model. To test the effect of the restrictions on the thermodynamic properties of the model water, we have simulated additionally the isobar  $P = 0$  in the restricted NPT ensemble for the ST2 model from 200 to 450 K. Liquid densities obtained by this method were compared with the saturated liquid densities, obtained by GEMC simulations.

Since neither the location of the liquid-liquid phase transitions (except for one transition of the ST2RF model [5, 6, 9, 20, 21, 22]) nor even their number are known *a priori*, we explored in detail a wide density interval (from 0.8 to  $1.4 \text{ g cm}^{-3}$ ) and pressure (from  $-6$  to  $+10$  kbar). To detect all branches of the studied isotherm, we performed simulations in the following way. Several configurations of liquid water with different densities were equilibrated in the restricted NVT ensemble. Then, each prepared configuration was used as an initial one for simulations in the restricted NPT ensemble at several chosen pressures. The systems converge to one (at supercritical temperatures) or more (at subcritical temperatures) densities, which correspond to all possible stable and metastable states of liquid water at the considered pressure and temperature. The density dependence of the isotherms in each detected water phase was studied by increasing (decreasing) the pressure in small steps (0.1 kbar in some cases). At some pressure, which roughly corresponds to the stability limit (spinodal), the

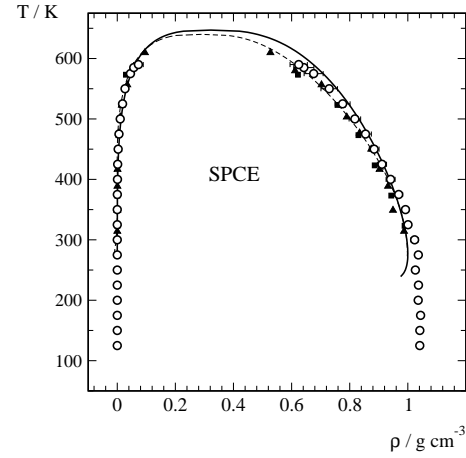


FIG. 5: Liquid-vapor coexistence curve of SPCE water model (open circles). Simulation data from Ref.[40], Ref.[41] and Ref.[42] are shown by dashed line, solid triangles and solid squares, respectively. Experimental data [27, 28] are shown by solid line.

density of a considered water phase in the course of a simulation run rapidly shifts to another branch of the isotherm, corresponding to another water phase. This approach should allow for discovering all branches of a water isotherm, whose densities at the same pressure differ more than about  $0.03 \text{ g cm}^{-3}$ . This value approximately corresponds to the thermodynamic fluctuations of the density in our finite system.

The obtained isotherms do not allow to locate accurately the coexistence pressure and the densities of the coexisting phases due to the missing parts in the region of the unstable states. Moreover, the density is not necessarily the appropriate order parameter to describe the liquid-liquid phase transition of a one-component system. Therefore, we attributed the coexistence pressure to the average of the maximal and minimal pressures of the overlap region, where the two branches have two distinct densities at the same pressure. Above the glass transition temperature  $T_g$ , the accuracy of such estimates is comparable with the accuracy of the simulated densities. Far below  $T_g$ , the density ranges of the different branches of the isotherm strongly overlap and the densities of the coexisting phases can be estimated only very roughly. Note, that at  $T < T_g$ , we do not infer from abrupt variations of the density in a small pressure interval to the existence of some phase transition. Additional information about the sign of the coexistence pressure we can obtain by attributing the density of the liquid branch of the liquid-vapor coexistence curve at the same temperature to zero pressure.

### III. RESULTS

#### A. Liquid-vapor coexistence of water from the critical point to the glassy state

##### 1. Liquid density along the liquid-vapor coexistence curve

The liquid-vapor coexistence curves of the ST 2 and ST 2RF water models are shown in Fig. 1. In both models at high temperature the liquid densities are essentially lower than the experimental values due to the strongly underestimated critical temperatures  $T_c$  (see Table I). At ambient temperatures the liquid density of the ST 2 model is close to the density of real water, whereas in the ST 2RF model it remains significantly underestimated (Fig. 2). Our results of the GEMC simulations (Fig. 2) agree well with the results of molecular dynamics (MD) simulations of the ST 2 [29] and ST 2RF [6] models at  $P = 0$ . The ST 2 model shows the density maximum at about 305 K and reproduces the experimental liquid density well in a temperature range of about 70 , when the latter is shifted upwards by 28 (see Fig. 2). At all temperatures the liquid density of the ST 2RF model is significantly below the experimental values. The temperature  $T_{max}$  of the density maximum in the ST 2RF model (about 320 K) is slightly higher than in the ST 2 water, and the absolute value of the liquid density  $\rho_1$  is about 7% below the experimental value. The experimental density  $\rho_1$  of about  $1 \text{ g cm}^{-3}$  can be reproduced in the ST 2RF model by applying a positive pressure of about 800 bars [5, 25]. The drastic density difference between ST 2 and ST 2RF models is caused by the application of the reaction field method for the treatment of the LRCI corrections in the latter case, which apparently strengthens the water hydrogen bonding. The shift of the liquid density in the ST 2RF model agrees with the predictions of the modified van der Waals model for water [43]. The characteristic temperature interval from  $T_c$  to  $T_{max}$  is only 66% of experimental value for the ST 2 model and only 58% for the ST 2RF model (Table I). Note, that in both models a density minimum follows the density maximum with decreasing temperature (see Figs. 1 and 2).

The striking feature of the liquid-vapor coexistence curve of the ST 2 model is a break of the liquid branch at  $T = 270 \text{ K}$  (Figs. 1 and 2). At this temperature two liquid phases with different densities (about 0.91 and  $0.97 \text{ g cm}^{-3}$ ) coexist with the vapor phase. This is not the case for any other studied temperatures, including the nearest ones  $T = 265 \text{ K}$  and  $T = 275 \text{ K}$ , where only one liquid phase coexists with the vapor. Evidently, there is a triple point at  $T = 270 \text{ K}$ , where two first order phase transitions (liquid-vapor and liquid-liquid) meet each other. The gradual change of  $\rho_1$  of the ST 2RF model in the whole studied temperature range (Fig. 2) indicates the absence of the triple point in this model. The disappearance of the triple point with the strengthening of the water hydrogen bonding qualitatively agrees with the predictions of the modified van der Waals model for water [43].

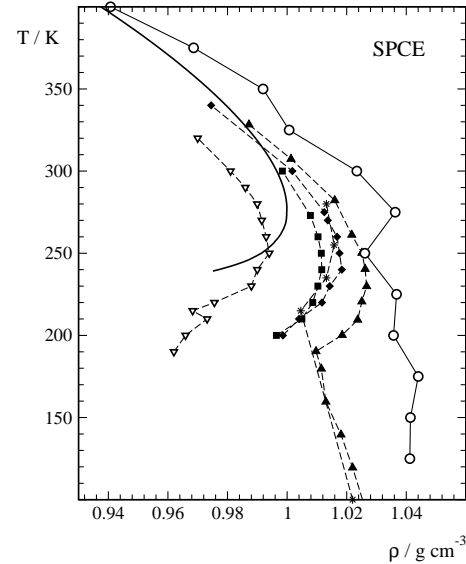


FIG. 6: Liquid densities of the SPCE water model along the liquid-vapor coexistence curve (open circles). Simulation data at  $P = 0$ : triangles up [44], triangles down [45], squares [46], stars [47] and diamonds [48]. Experimental data [27, 28] are shown by the solid line.

The liquid-vapor coexistence curves of the TIP 4P and TIP 5P water models are compared with the experimental data in Fig. 3. On cooling the liquid density in both models passes through a maximum and afterward through a minimum. Both models underestimate the critical temperature (Table I), that essentially depresses liquid density at high temperatures, especially in the case of the TIP 5P model. For the TIP 4P water model the characteristic temperature interval from  $T_c$  to  $T_{max}$  is about 88% of the experimental value, whereas for the TIP 5P model it is only 70%, which is close to the value for the other five-site water model, the ST 2 model (see Table I). Most of the data points for the TIP 4P model are from our previous paper [34], where comparisons with other simulation studies of the coexistence curve can be found (see Fig. 5 in Ref. [34]). Depending on the implementation of the TIP 4P and TIP 5P water models (long-range corrections for intermolecular interactions, cutoff, system size, etc.), the density of the saturated liquid varies within 1–2 %. In particular, using the LRCI corrections causes a slight decrease of liquid density, whereas including the LRLJ corrections causes the opposite trend.

The details of the particular implementation of the water model and the employed simulation method gain more importance at low temperatures (Fig. 4). At ambient temperatures the liquid density of the TIP 4P water model is not very sensitive to the simulation details. However, in the supercooled region two different courses of the liquid density are obtained: in our simulation  $\rho_1$  starts to increase with decreasing temperature at  $T < 225 \text{ K}$ , whereas in other simulations [6, 37] it continues to decrease. Apparently, this difference is caused by the

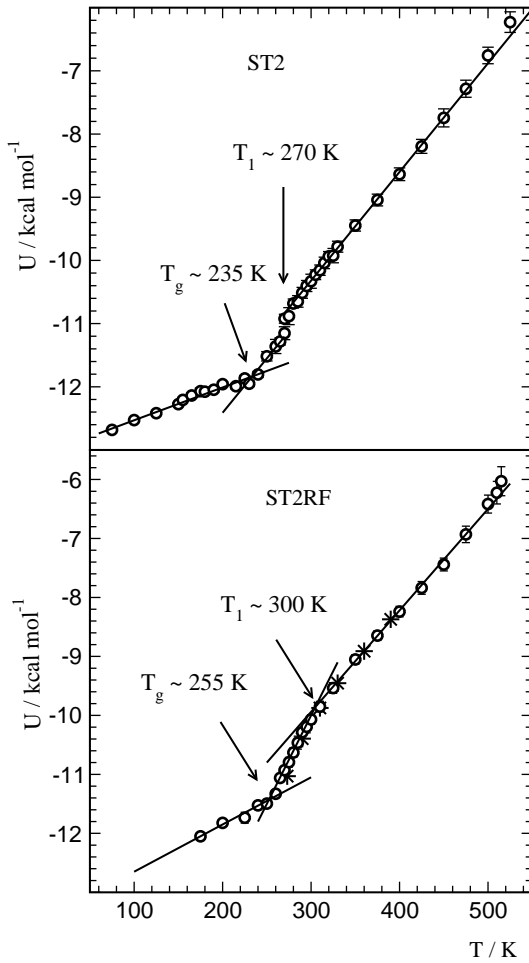


FIG. 7: Potential energy  $U$  in the liquid phase along the liquid-vapor coexistence curve of the ST 2 and ST 2RF water models (open circles). The values of  $U$ , obtained from simulations of the ST 2RF model at  $P = 0$  [6], are shown by stars.

use of LRLJ corrections in the former case and by the application of LRCI corrections in the latter case.

The TIP5P water model seems to be more sensitive to the simulation details [35, 49, 50]. In the region of the density maximum the use of LRCI corrections [35] causes a decrease of  $\rho_1$  by about 2%, whereas the use of LRLJ corrections (our simulations) causes a slight increase of  $\rho_1$  in comparison with the original TIP5P model [31], which was parameterized without any long-range corrections for intermolecular interactions (Fig. 4). In the supercooled region the increase of  $\rho_1$  due to the LRLJ corrections achieves about 3%.

Among the considered water models, the SPCE model gives the most realistic value of  $T_c$  (see Table I), and therefore the simulated and experimental values of the coexisting densities are close at high temperatures (Fig. 5). The characteristic temperature interval from  $T_c$  to  $T_{\max}$  is also close to the experimental value (Table I). Application of the LRCI corrections [40, 41, 42] depresses the liquid density by about 2–3% similarly to other water

models. At low temperatures the behavior of the density of the saturated liquid in the SPCE model seems to be more sensitive to the simulation details in comparison with other models (Fig. 6). In the region of the density maximum the value of  $\rho_1$  is largest, when only LRLJ corrections are taken into account (Fig. 6, circles). It subsequently decreases, when such corrections are excluded (Fig. 6, solid triangles), when both kinds of the long-range corrections are included (Fig. 6, diamonds) and when only LRCI corrections are included (Fig. 6, squares). The use of a smaller spherical cutoff results in the lowest liquid density (Fig. 6, open triangles).

Some features of the temperature dependence of the saturated liquid density at ambient and supercooled temperatures seem to be general for all studied water models, despite the high sensitivity of the phase diagram to the model and its implementation. All studied water models show the well-known density maximum (see Table I). This maximum is followed by a density minimum with decreasing temperature. Previously, we observed the liquid density minimum along the liquid-vapor coexistence curve for TIP4P water [34, 51, 52] (Figs. 3 and 4), ST2 water [10] (Figs. 1 and 2) and TIP5P water [11] (Figs. 3 and 4). Now, the ST2RF water model also shows a pronounced density minimum (Figs. 1 and 2). Although we are not able to locate both a density minimum and a maximum in our simulations of SPCE water (Fig. 5), the existence of the density minimum seems to be quite possible for other implementations of this model (Fig. 6). Note, that the liquid density minimum around 185–195 K was also observed upon temperature quench of a water model, proposed by Guillet and Guissani [53].

## 2. Potential energy of liquid water along the liquid-vapor coexistence curve and glass transition

The temperature dependence of the potential energy  $U$  of the water molecules in the along the liquid-vapor coexistence curve is shown in Fig. 7 for the ST2 model. The discontinuity of  $U$  (of about 0.23 kcal/mol) at  $T = 270$  K reflects the liquid-liquid phase transition at the triple point. The slope of  $U(T)$  does not change noticeably when crossing the triple point, indicating the essentially liquid nature of the coexisting phases. A slower change of  $U(T)$ , typical for the glassy state, is observed at low temperatures. This allows an estimate of the glass transition temperature of the ST2 water model at zero pressure as  $T_g = 235$  K.

The temperature dependence of the potential energy  $U$  of the ST2RF water model indicates a transition to the glassy state at  $T_g = 255$  K, i.e. slightly higher than in the ST2 model. Two different slopes of  $U(T)$  above  $T_g$  evidences two quite different kinds of liquid water. The continuous transition between these two liquids occurs at about 300 K, i.e. about 20 below the temperature of the density maximum (Fig. 7, Table I).

Transitions to glassy states are also seen for the TIP4P

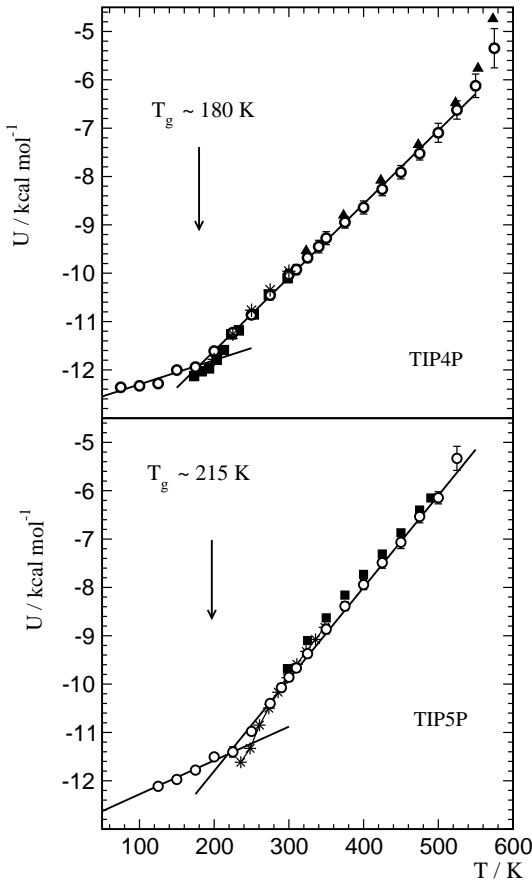


FIG. 8: Potential energy  $U$  in the liquid phase along the liquid-vapor coexistence curve of the TIP4P and TIP5P water models (open circles). The values of  $U$ , obtained from simulations at  $P = 0$  are shown by squares [37], stars [6] and triangles [42].

and TIP5P water models (circles, Fig.8). The estimated values of the glass transition temperature are:  $T_g = 180$  K for the TIP4P model and  $T_g = 215$  K for the TIP5P model. Note, that the use of the LRCI correction (Fig.8, squares and stars in the upper panel and stars in the lower panel) results in noticeably lower potential energies at  $T = 225$  K for the TIP4P model and  $T = 275$  K for the TIP5P model. This is obviously connected with the essentially different densities of water in the two implementations of the TIP4P and TIP5P water models at  $T = 225$  K and  $T = 275$  K, respectively (see Fig.4). The glass transition temperature of the SPCE water model noticeably depends on its implementation (see Table I) and in our simulation study the glass transition temperature  $T_g = 220$  K for this model (Fig.9).

### 3. Heat capacity along the liquid-vapor coexistence curve

The heat capacity at constant pressure  $C_p$  is the temperature derivative of the enthalpy and relates to the

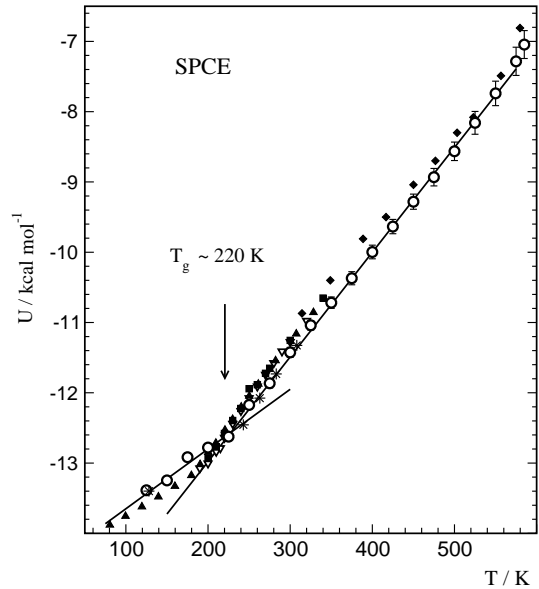


FIG. 9: Potential energy  $U$  in the liquid phase along the liquid-vapor coexistence curve of the SPCE water model (open circles). Values of  $U$ , obtained from simulations at  $P = 0$ : triangles up [44], triangles down [45], squares [46], stars [47] and diamonds [41].

potential energy of a system through the equation:

$$C_p = \frac{\frac{\partial (U + PV + 3RT)}{\partial T}}{P} : \quad (2)$$

Along the liquid-vapor coexistence curve, the contribution of  $P(\partial V/\partial T)_P$  to  $C_p$  is negligible up to temperatures of about 450 to 500 K. We have computed  $C_p$  by central difference of the internal energy  $U + 3RT$ . The data for the lowest and the highest temperature were estimated using the forward and backward formulas for the derivative, respectively.

Our simulation results are compared with the experimental data and other simulation studies of  $C_p$  in Figs.10 and 11. The value of  $C_p$  of the high-temperature liquid is about twice the  $C_p$  in the glassy state. The temperature dependence of  $C_p$  differs substantially in the different water models. The heat capacity of the ST2 model shows a shallow minimum at about 375 K and a sharp maximum near 270 K, i.e. near the triple point of the liquid-vapor and liquid-liquid phase transition (Fig.10, upper panel). The values of  $C_p$  of both liquid phases below and above 270 K are comparable (about  $0.026 \text{ kcal mol}^{-1} \text{ K}^{-1}$ ). The ST2RF model shows a gradual increase of  $C_p$  upon cooling in a wide temperature range (Fig.10, lower panel). At 300 K, where a gradual transition between two forms of liquid water occurs,  $C_p$  increases abruptly to a value of about  $0.04 \text{ kcal mol}^{-1} \text{ K}^{-1}$ , and remains at such high values till the transition to a glassy state. So, the heat capacity of the second (low-temperature) liquid in the ST2RF model is almost two times higher, than the heat capacity of the ordinary liquid, which coexists

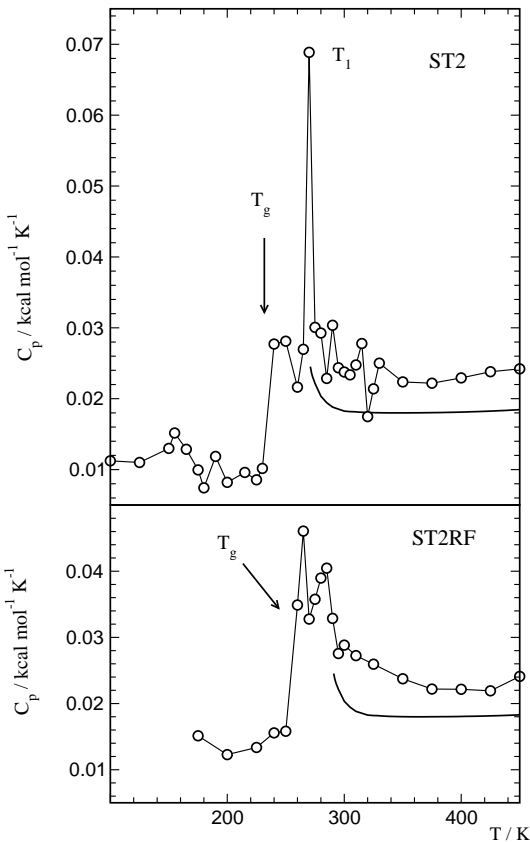


FIG. 10: Heat capacity of liquid water along the liquid-vapor coexistence curve: our simulation (open circles) and experiment [18, 27] (thick lines). Experimental data are shifted by +35 and +55 for comparison with the ST 2 and ST 2RF water models, respectively.

with the vapor in a wide temperature range up to the liquid-vapor critical point.

The absolute values of  $C_p$  in the TIP4P and SPC-E water models are rather close to the experimental data in a wide temperature range (Fig.11). Although a slight increase of  $C_p$  in the TIP4P model is observed upon cooling, its gradual character differs essentially from the sharp increase of  $C_p$  in a narrow temperature range, observed experimentally. The SPC-E model does not show a noticeable increase of  $C_p$  upon cooling. Similarly to the ST 2 and ST 2RF models, the TIP5P water model noticeably overestimates  $C_p$  in a wide temperature range. It shows a gradual increase of  $C_p$  in a wide temperature range upon cooling, interrupted by the onset of a glassy state.

## B. Liquid-liquid phase transitions of water at low temperatures

### 1. ST 2 model

Isotherms of the ST 2 water model, obtained by MC simulations in the restricted NPT ensemble at  $T = 200$  to  $290$  K, are shown in Figs.12 and 13. No liquid-liquid transitions could be detected at  $T = 290$  K, where the liquid density gradually changes with pressure. At  $T = 275$  K a liquid-liquid coexistence appears at slightly negative pressure ( $P = -0.2$  kbar) and the densities of the coexisting liquid phases are about  $0.94$  and  $0.98$  g cm $^{-3}$ . At  $T = 260$  K this transition shifts to positive pressure ( $P = +0.4$  kbar) and the two-phase region becomes wider (from about  $0.90$  to  $1.01$  g cm $^{-3}$ ). So, at some temperature between  $275$  K and  $260$  K this liquid-liquid transition should pass through zero pressure, i.e. should meet the liquid-vapor phase transition at a triple point. Indeed, such a triple point at  $T = 270$  K was found at the liquid-vapor coexistence curve of the ST 2 model (Figs.1 and 2). The densities of the coexisting liquid phases at the triple point, estimated from the GEMC simulations of the liquid-vapor coexistence,  $0.91$  and  $0.97$  g cm $^{-3}$ , are in good agreement with the MC simulations in the restricted NPT ensemble. Moreover, extensive direct equilibration of the two liquid phases in the Gibbs ensemble also gives a rather similar coexistence region: between  $0.92$  and  $1.00$  g cm $^{-3}$  at  $T = 270$  K and between  $0.90$  and  $1.02$  g cm $^{-3}$  at  $T = 260$  K (see Fig.4 in Ref.[10]). With decreasing temperature to  $T = 235$  K neither the pressure nor the densities of these coexisting phases change noticeably. At  $T = 200$  K (Fig.13) this transition is still visible at positive pressures and approximately in the same density range.

The ST 2 water model shows at  $T = 260$  K a second liquid-liquid phase transition, occurring at positive pressure ( $P = +0.5$  kbar) in the density interval from  $1.02$  to  $1.11$  g cm $^{-3}$ . This interval agrees well with the densities of the coexisting phases, obtained directly in GEMC simulations:  $1.03$  and  $1.12$  g cm $^{-3}$  at  $T = 270$  K and  $1.04$  and  $1.12$  g cm $^{-3}$  at  $T = 260$  K (Fig.4 in Ref.[10]). The densities of the coexisting phases do not change noticeably at  $T = 235$  K, whereas the coexistence pressure slightly increases up to  $P = +0.85$  kbar. The complexity of the isotherm of ST 2 water obtained for  $T = 200$  K (Fig.13) makes it difficult to identify this transition at such a low temperature. A third liquid-liquid phase transition of the ST 2 water model appears at  $T = 235$  K. It is located at positive pressure ( $P = +0.95$  kbar) (Fig.12) and the densities of the coexisting liquid phases are  $1.12$  and  $1.19$  g cm $^{-3}$ .

The location of the thus observed liquid-liquid coexistence regions with respect to the liquid branch of the liquid-vapor coexistence curve is shown schematically in Fig.14 (upper panel). The simulation results evidence, that the first (the lowest-density) liquid-liquid phase transition of the ST 2 model should have a criti-

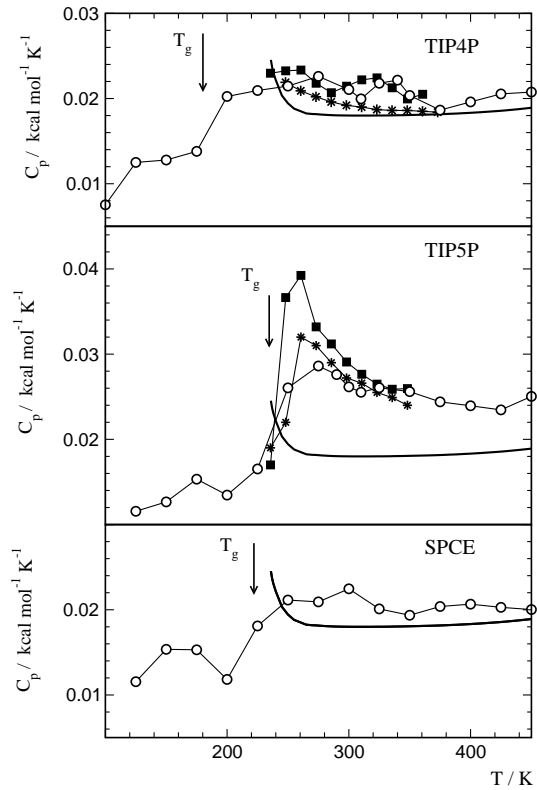


FIG. 11: Heat capacity of liquid water along the liquid-vapor coexistence curve: our simulation (open circles) and experiment [18, 27] (thick lines). Data from other simulation studies at  $P = 0$ : TIP4P model [38] (squares, upper panel), TIP4P-Ew model [50] (stars, upper panel), TIP5P model [31] (squares, middle panel), TIP5P-Ew model [49] (stars, middle panel)

cal point of demixing at slightly negative pressures with a critical temperature between 275 K and 290 K and a critical density between 0.94 and 0.98 g cm<sup>-3</sup>. It seems likely, that the second and third phase transitions also end at corresponding critical points. However, the observed temperature evolution of the coexisting densities of these transitions does not allow to exclude the possibility of a common critical point. If so, the narrow one-phase region near 1.1 g cm<sup>-3</sup> should end in a triple point, where three liquid phases coexist. Note, that all three phase transitions occur above the glass transition temperature  $T_g = 235$  K, estimated at zero pressure. This means, that at least the first transition is a transition between two liquid phases. The complexity of the isotherm at  $T = 200$  K (Fig. 13) obviously indicates the appearance of several coexisting glassy and possibly some crystalline phases. This complex behavior may reflect the experimental observation of a multitude of amorphous ice structures with nearly continuous transitions [54]. The structure of these phases has to be studied to clarify their nature.

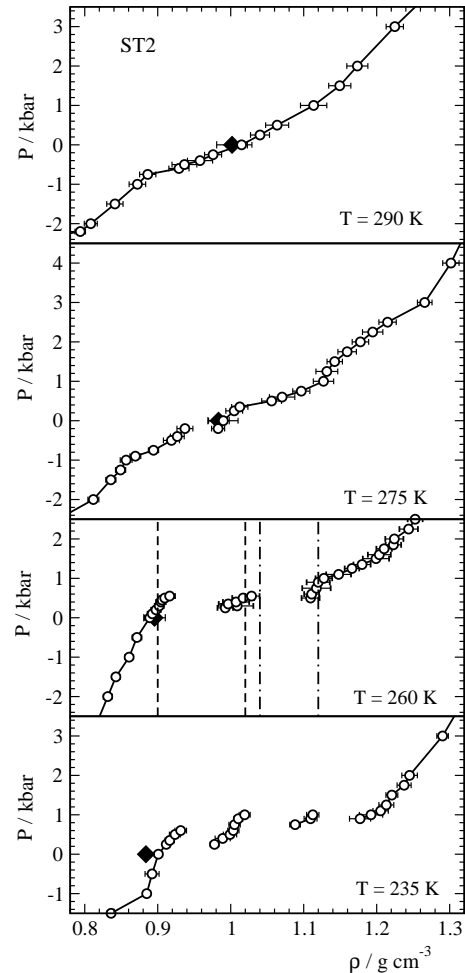


FIG. 12: Isotherms of ST2 water (open circles) and densities of the liquid phase at the liquid-vapor coexistence curve (diamonds at  $P = 0$  bar). The densities of the coexisting phases of the first and second liquid-liquid phase transitions of ST2 water at 260 K, obtained by GEMC simulations, are shown by dashed and dot-dashed lines, respectively.

## 2. ST2RF model

Several isotherms of the ST2RF water model, obtained by MC simulations in the restricted NPT ensemble at  $T = 200$  to 290 K, are shown in Figs. 15 and 16 together with the results of other simulation studies. There is good agreement of our data for supercritical isotherms with MD simulations in the NVT ensemble (Fig. 15,  $T = 290$  and 275 K). In this water model the first liquid-liquid phase transition appears at  $T = 260$  K and  $P = 1.3$  kbar in the density interval from 0.94 to 1.01 g cm<sup>-3</sup>. The shape of the isotherm indicates a critical point at positive pressure slightly above 260 K. The shift of the critical point from negative pressure for ST2 model to positive pressure for ST2RF model corroborates the expected changes of the water phase diagram with strengthening of the hydrogen bonding [43]. At  $T = 235$  K the two-phase region becomes wider (from 0.94 to

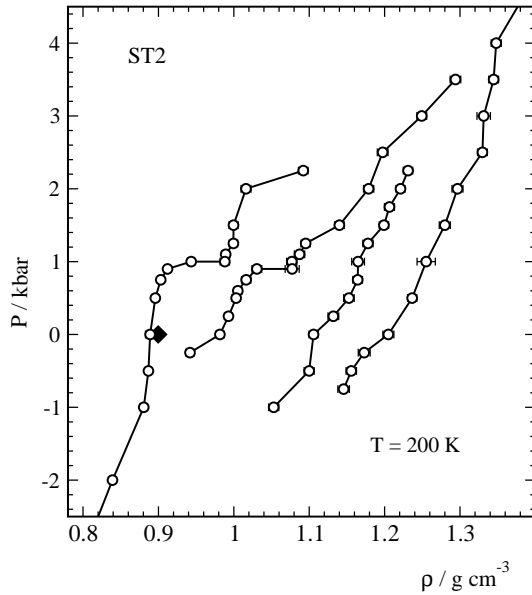


FIG. 13: Isotherm of ST 2 water at  $T = 200$  K (open circles) and density of the liquid phase at the liquid-vapor coexistence curve (diamonds at  $P = 0$ ).

1.10 g cm<sup>-3</sup>) and the coexistence pressure increases to  $P = +2.0$  kbar. Our isotherm at  $T = 235$  K agrees well with the results of other simulation studies (Fig.16). The systematic shift of the data points, obtained from a sedimentation profile [2], toward higher pressures is caused by a slightly lower temperature (230 K) and the absence of the LRLJ corrections in that study.

The first liquid-liquid phase transition of the ST 2RF model clearly reflects in the  $T = 200$  K isotherm, i.e. deeply below the glass transition temperature  $T_g = 255$  K, estimated at zero pressure. Probably due to this fact the density intervals of the different branches of the isotherm start to overlap (Fig.15, lower panel). This essentially complicates estimating the coexisting densities and the pressure at the transition. However, this transition remains roughly in the same pressure and density interval, as at  $T = 235$  K. The disappearance of the triple point with the strengthening of the water hydrogen bonding qualitatively agrees with the predictions of the model van der Waals model for water [43].

At  $T = 200$  K the ST 2RF model shows a pronounced second liquid-liquid (or better amorphous-amorphous) transition at  $P = +3$  kbar with a two-phase region roughly from 1.1 to 1.2 g cm<sup>-3</sup>. Schematically the location of the observed coexistence regions with respect to the liquid branch of the liquid-vapor coexistence curve of the ST 2RF model is shown in Fig.14 (lower panel). Note, that the density intervals of the second transition of the ST 2RF model and the third transition of the ST 2 model are very close. The coexistence region of the first transition of the ST 2RF model covers the two coexistence regions of the the first and second transitions of the ST 2 model.

### 3. TIP 4P model

The  $T = 200$  K isotherm of the TIP 4P water model shows a liquid-liquid phase transition in the density interval from 1.05 to 1.08 g cm<sup>-3</sup> (Fig.17). The critical point of this transition should be located slightly above 200 K, at  $P = +1$  kbar and  $1.06$  g cm<sup>-3</sup>. Continuous isotherms of TIP 4P water were obtained in MD simulations using the NVT [6] and NPT [24] ensembles (see stars and triangles, respectively, in Fig.17). The shift of the MD data to lower densities may be attributed to the use of LRCI corrections in Refs.[6, 24]. The compressibility maximum, obtained in the MD simulations Refs.[6] and [21] at  $1.03$  g cm<sup>-3</sup> is rather close to the critical density at  $1.06$  g cm<sup>-3</sup> in our simulations. The absence of the liquid-liquid transition at  $T = 200$  K in the MD simulation studies Refs.[6] and [24] should be attributed to the shortcomings of the applied simulation methods, which underestimate the critical temperature (see Introduction).

When decreasing the temperature to 175 K, two liquid-liquid phase transitions are seen. The first one is located at  $P = -0.8$  kbar with densities of the coexisting phases of 0.96 and 1.02 g cm<sup>-3</sup>. This transition is located in the metastable region with respect to evaporation (see diamonds in Fig.17). Decreasing further the temperature to  $T = 150$  K, which is essentially below the glass transition temperature  $T_g = 180$  K, estimated at zero pressure, the different branches of the isotherm overlap in a wide range of pressure and density (Fig.17, lower panel). At  $T = 150$  K the first transition apparently remains at negative pressure and its parameters seem to be close to the one at  $T = 175$  K. At  $T = 175$  K the second liquid-liquid transition of the TIP 4P water model occurs at  $P = +1.8$  kbar with densities of the coexisting phases of 1.08 and 1.14 g cm<sup>-3</sup> (Fig.17, middle panel). When decreasing the temperature to 150 K, the two-phase region becomes wider and extends up to 1.2 g cm<sup>-3</sup> (Fig.17, lower panel).

The liquid branch of the liquid-vapor coexistence curve of the TIP 4P model varies smoothly with temperature and does not show any triple point (Figs.3,4). Therefore, the first liquid-liquid transition, which occurs at a negative pressure at  $T = 150$  and 175 K, should end with a critical point between 175 and 200 K also at negative pressure.

The location of the two liquid-liquid transitions with the respect to the liquid branch of the liquid-vapor coexistence curve of the TIP 4P model is shown schematically in Fig.18. The results of MD simulations of supercooled TIP 4P model [6, 21, 24] do not contradict to this picture. Indeed, the drop of the water density from about 1.12 to 1.05 g cm<sup>-3</sup> between 193 and 173 K along the isobar  $P = 2$  kbar in ref. [24], is caused by crossing the second liquid-liquid transition of TIP 4P water (Fig.18). The sharp change of the water density along the isobar  $P = 0$  [24] probably reflects the proximity of the first liquid-liquid phase transition, which in that implemen-

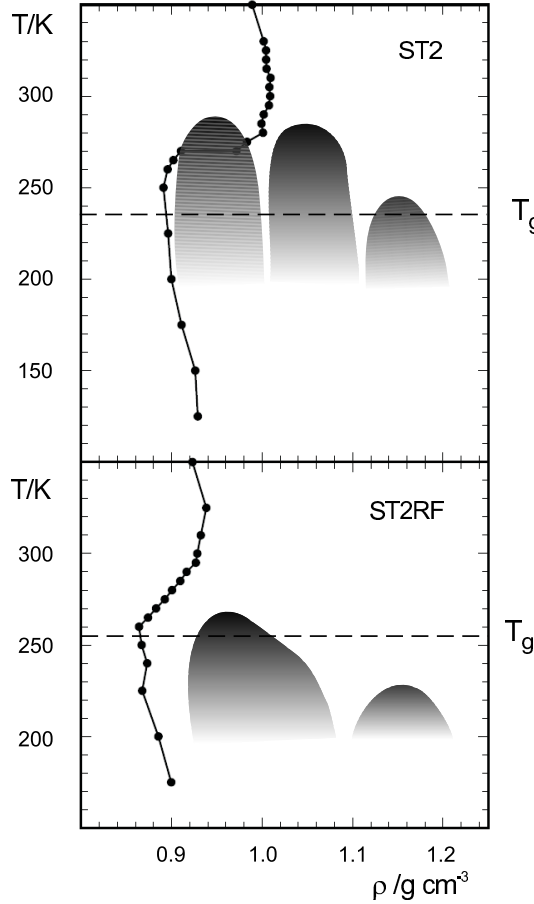


FIG. 14: Location of the liquid-liquid phase transitions (shaded areas) with respect to the liquid branch of the liquid-vapor coexistence curve (solid circles) for the ST 2 and ST 2RF water models. Glass temperature at  $P = 0$  is indicated by dashed line.

tation of the TIP 4P model may be located at slightly positive pressures (see squares in Fig.4).

#### 4. TIP 5P model

Isotherms of the TIP 5P water model at supercooled temperatures are shown in Fig.19. The inception point of the  $T = 250$  K isotherm of the TIP 5P model is located approximately at the same pressure and density, as the inception point of the  $T = 200$  K isotherm of the TIP 4P model (Fig.17). Note, that a similar shape of this isotherm was obtained from MD simulations in the NVT ensemble [8]. At  $T = 225$  K a liquid-liquid phase transition appears at  $P = +1.3$  kbar with densities of the coexisting phases  $1.03$  and  $1.08$   $\text{g cm}^{-3}$ . This transition was not observed at this temperature in MD simulations [8], probably due to the unavoidable distortion of the subcritical isotherms, obtained in the NVT ensemble. With decreasing temperature the coexistence pressure of this transition increases noticeably and the

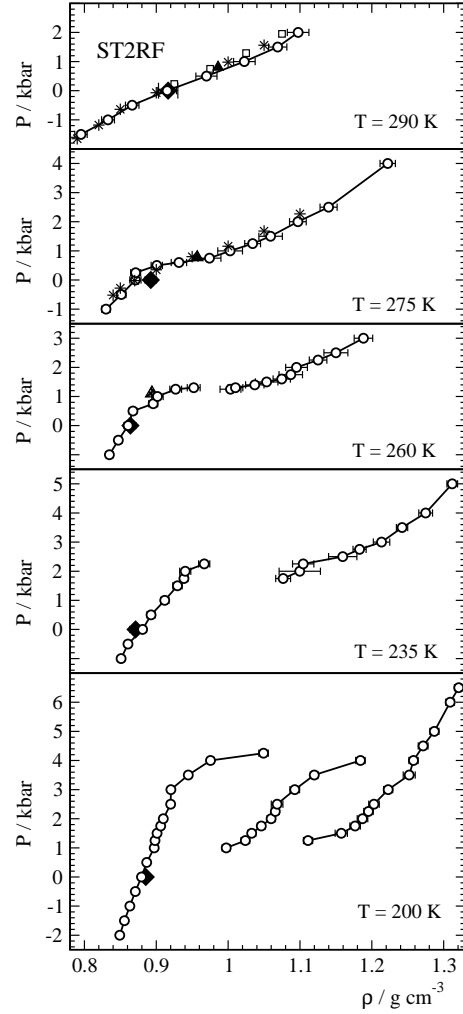


FIG. 15: Isotherms of ST 2RF water from MC simulations in the restricted NPT ensemble (open circles) and densities of the liquid phase at the liquid-vapor coexistence curve (diamonds at  $P = 0$  bar). Data points from MD simulations in the NVT ensemble are shown by stars [6], open squares [7] and solid triangles [25].

densities of both coexisting phases shift to higher values.

A lower-density liquid-liquid transition appears at  $T = 175$  K with densities of the coexisting phases  $0.99$  and  $1.03$   $\text{g cm}^{-3}$ . Obviously, this transition appears at slightly positive pressure (see the location of the liquid density at the liquid-vapor coexistence curve at  $T = 175$  K indicated by a diamond in Fig.19). At  $T = 150$  K this transition is observed at negative pressures (about  $-3$  kbar) in the density interval from  $0.94$  to  $0.99$   $\text{g cm}^{-3}$ . So, this liquid-liquid transition should cross the liquid-vapor coexistence curve at a triple point between  $150$  and  $175$  K. Indeed, a sharp change of the liquid density at the liquid-vapor coexistence curve is observed at this temperature interval (see Fig.4). The location of the estimated liquid-liquid two-phase regions with the respect to the liquid branch of the liquid-vapor coexis-

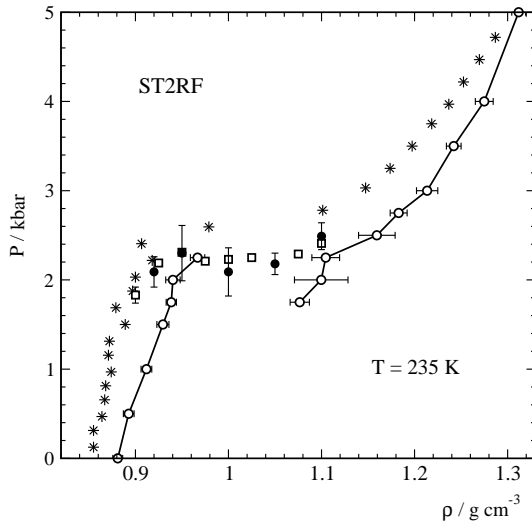


FIG. 16: Isotherm of ST2RF water at  $T = 235$  K from MC simulations in the restricted NPT ensemble (open circles) and from MD simulations in the NVT ensemble (solid circles [6], squares [7]). The isotherm, obtained from a sedimentation profile at  $T = 230$  K [9] is shown by stars.

tence curve of the TIP5P model is shown schematically in Fig.18 (middle panel). Note some discrepancy between this phase diagram and the liquid-liquid phase transition with a critical point at  $T = 217$  K,  $P = 3.4$  kbar and  $\rho = 1.13$  g cm<sup>-3</sup>, estimated for the TIP5P model in Ref.[8].

### 5. SPCE model

The appearance of a liquid-liquid (or better amorphous-amorphous) phase transition of the SPCE model is seen from the isotherm  $T = 200$  K (Fig.20). The critical point of this transition we estimate at temperature slightly above 200 K,  $P = +0.9$  kbar and  $1.06$  g cm<sup>-3</sup>. With decreasing temperature the coexistence pressure of this transition remains positive, whereas the density range of the two-phase coexistence increases from  $1.07 - 1.13$  g cm<sup>-3</sup> at  $T = 175$  K to  $1.09 - 1.16$  g cm<sup>-3</sup> at  $T = 150$  K. The lower-density liquid-liquid phase transition appears at slightly negative pressure, the coexistence region we estimate as  $0.99 - 1.04$  g cm<sup>-3</sup> at  $T = 175$  K and  $0.97 - 1.03$  g cm<sup>-3</sup> at  $T = 150$  K. The location of these two liquid-liquid transitions with respect to the liquid branch of the liquid-vapor coexistence curve is shown schematically in Fig.18. Studies of the liquid-liquid transition of the SPCE model, based on an analytic expansion for the liquid free energy [57] do not agree with our phase diagram. First, the existence of a single liquid-liquid transition was proposed in Ref.[57]. The critical point of this single liquid-liquid transition, estimated at  $T = 130$  K,  $P = +2.9$  kbar and  $\rho = 1.10$  g cm<sup>-3</sup>, is essentially shifted to lower temperature and higher pressure in comparison with the critical points of the two liquid-liquid phase

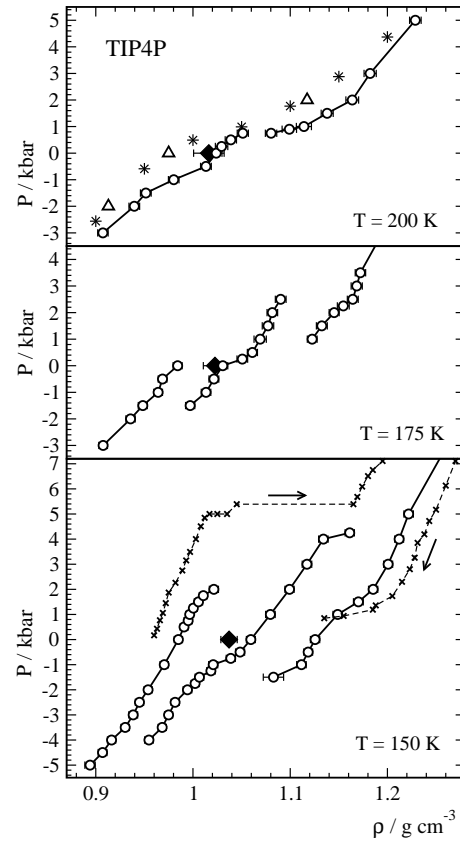


FIG. 17: Isotherms of TIP4P water from MC simulations in the restricted NPT ensemble (open circles) and densities of the liquid phase at the liquid-vapor coexistence curve (diamonds at  $P = 0$  bar). Data points from MD simulations in the NVT ensemble [6] are shown by stars and from MD simulations in the NPT ensemble at  $T = 193$  K [24] are shown by triangles. Experimental data points, corresponding to the transition between low-density and high-density amorphous ice at  $T = 110$  K [55, 56], are shown by crosses. Arrows indicate compression and decompression.

transitions, shown in Fig.18. This shift is probably caused by the use of LRCI corrections in Ref.[57].

### IV. DISCUSSION

Phase transitions between two liquid or amorphous phases with different densities were observed for several water models by simulations in the restricted NPT ensemble. The reliability of the applied method was tested by direct GEMC simulations of the liquid-vapor and liquid-liquid coexistence of ST2 water. In particular, the  $P = 0$  isobar simulated in the restricted NPT ensemble from the supercooled region up to  $T = 450$  K well agrees with the liquid branch of the liquid-vapor coexistence curve obtained by GEMC simulations [10]. The triple point of this model, where the water vapor coexists with two different liquid water phases, was obtained by three different methods: simulations in the restricted

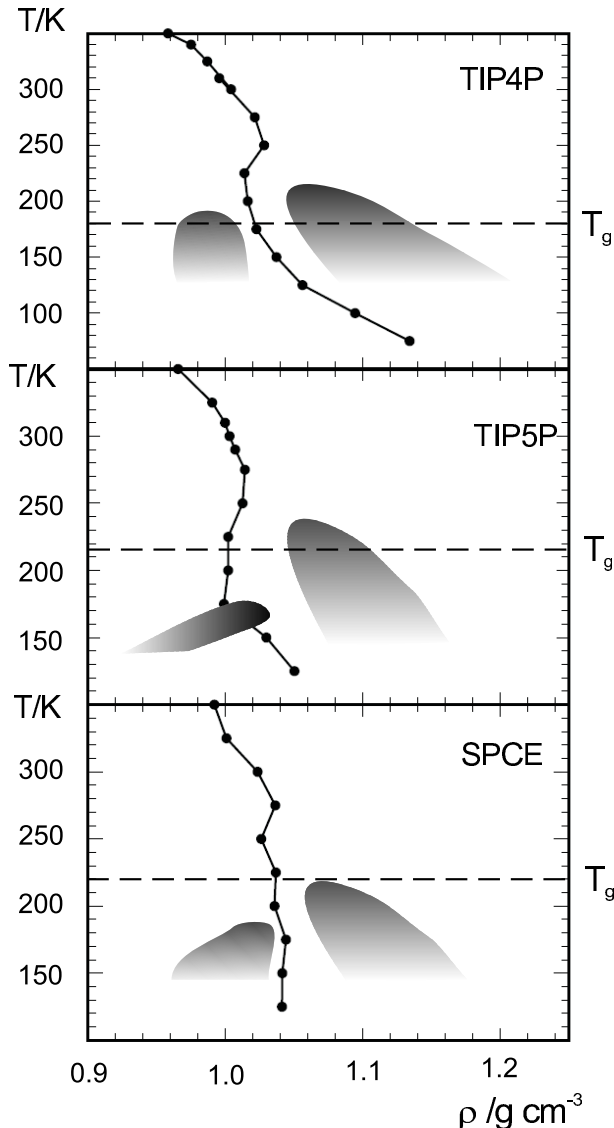


FIG . 18: Schematic representation of the location of the liquid-liquid phase transitions (shadowed areas) with respect to the liquid branch of the liquid-vapor coexistence curve (solid circles) for TIP4P, TIP5P and SPCE water models. Glass temperature at  $P = 0$  bar is indicated by dashed line.

NPT ensemble and simulations of the liquid-vapor and liquid-liquid coexistence in the Gibbs ensemble.

There is a general agreement of our simulation results with available simulation studies of the same water models. Discrepancies are connected mainly with the differences in implementation of the water model. In particular, the use of long-range corrections for the intermolecular interaction in water models, which were parameterized without any long-range corrections, essentially affects the liquid density. The use of LRCI corrections causes a decrease of the liquid density especially at low temperatures. This effect is most dramatic for the ST2 water model and therefore we consider in fact two water

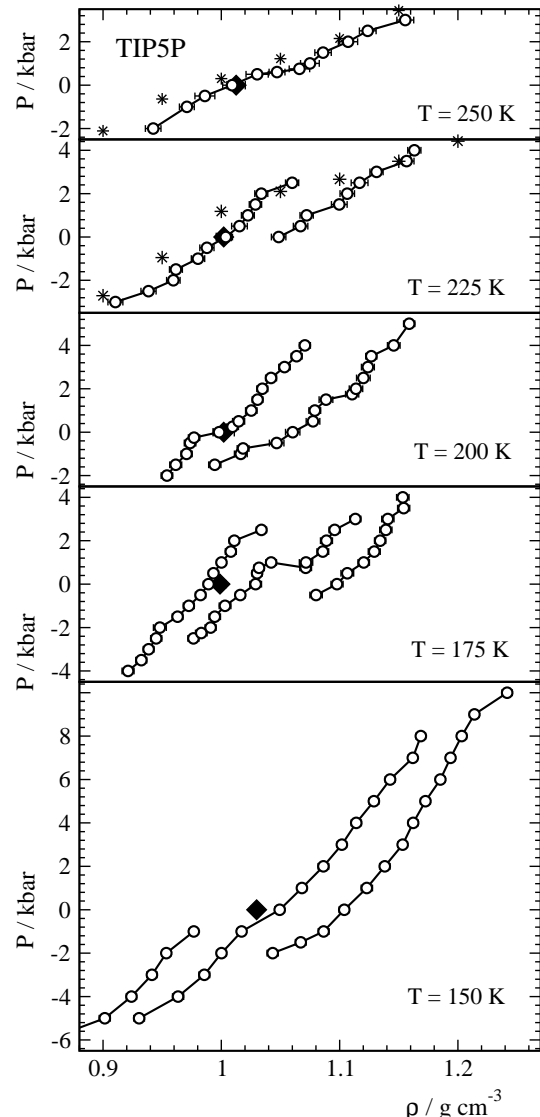


FIG . 19: Isotherms of TIP5P water from MC simulations in the restricted NPT ensemble (open circles) and densities of the liquid phase at the liquid-vapor coexistence curve (diamonds at  $P = 0$  bar). Data points from MD simulations in the NVT ensemble [8] are shown by stars (for  $T = 225$  K these points were obtained by interpolation of the data for  $T = 220$  and  $230$  K ).

models: ST2 and ST2RF. The use of LRLJ corrections results in the opposite effect, i.e. in an increase of the liquid density. Again, this effect enhances with decreasing temperature.

Another discrepancy between different simulation studies of supercooled water originates from the method, used for the detection (location) of the liquid-liquid phase transitions. Due to the intrinsic limitations of the simulations in the canonical NVT ensemble (see Introduction), this method noticeably underestimates the critical temperature of the phase transition. For example, in some temperature interval below the critical tem-

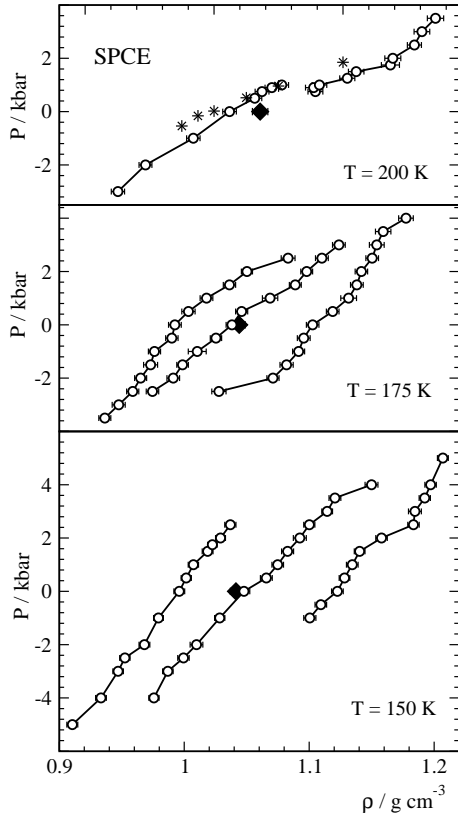


FIG. 20: Isotherms of SPCE water from MC simulations in the restricted NPT ensemble (open circles) and densities of the liquid phase at the liquid-vapor coexistence curve (diamonds at  $P = 0$  bar). Data points at  $T = 200$  K from MD simulations in the NVT ensemble [46] are shown by stars.

ature, where the simulations in the restricted ensemble evidence a phase transition, the isotherms, obtained in the NVT ensemble, look like supercritical (see Fig.17,  $T = 200$  K ; Fig.19,  $T = 225$  K ; Fig.20,  $T = 200$  K ). Note also, that the applicability of simulations in the NVT ensemble for the study of phase transitions is doubtful in the case of multiple phase transitions, which occur in a narrow pressure range (see, for example Fig.12,  $T = 235$  and  $260$  K ), due to unavoidable and unpredictable distortions of the subcritical isotherms.

The phase diagrams of the liquid-vapor and the liquid-liquid phase transitions are highly sensitive to the water model. All studied water models (except the ST 2RF model) show comparable liquid densities at ambient conditions, where all these models were parameterized. Both upon heating and cooling, these models show increasing deviations from the saturated liquid density. For instance, the liquid-vapor critical temperature  $T_c$  varies from 540 K to 640 K for the different water models (see Table I). The influence of the water model is even more obvious, when the distance between  $T_c$  and the temperature  $T_{\max}$  of the liquid density maximum is considered (Table I). This distance is largest and comparable with the experimental value for the three-site SPCE wa-

term model, whereas it is much smaller for five-sites water models (ST 2, ST 2RF and TIP 5P). Below  $T_{\max}$  and at supercooled temperatures the liquid density at the liquid-vapor coexistence curve and the densities of the coexisting liquid phases of the liquid-liquid phase transitions are highly sensitive to the water model and its implementation.

The multiplicity of liquid-liquid phase transitions, which we obtained for five non-polarizable models and Jedlovszky and Vallauri [12] obtained for a polarizable water model, seems to be more natural, than the existence of only one liquid-liquid transition. Obviously, these transitions are related to the variety of amorphous phases of the one-component isotropic fluid, which differ in their short-range local order. It is natural to assume, that each crystalline phase (or at least the crystalline phases, which can directly transform to the liquid phase) should result in a corresponding amorphous (liquid) phase with a short-range order, which is reminiscent of the crystalline phase [58, 59]. So, for water, showing at least 12 crystalline phases, 5 of which are in direct equilibrium with the liquid [60], a multiplicity of liquid-liquid phase transitions may be expected. This corroborates with the existence of at least 3 amorphous phases of supercooled water: low-density amorphous ice (LDA), high-density amorphous ice (HDA) [1] and very-high-density amorphous ice (VHDA) [61]. Moreover, the existence of other amorphous phases of supercooled water can not be excluded [54, 62].

The existence of more than one liquid-liquid phase transition in a one-component system was also concluded from simulation studies of other models [63, 64]. Two liquid-liquid phase transitions were found for a simple model system with a multistep shape of the intermolecular potential [63]. The number of steps directly determined the number of observed phase transitions. Two liquid-liquid phase transitions were also observed for a waterlike model confined between hydrophobic surfaces [64].

We have found three liquid-liquid phase transitions of the ST 2 water model. Hence, there are 4 distinct phases of supercooled water, which we have numbered as phase I to IV, starting from the phase with the lowest density. The density range, where the liquid-liquid transitions occur, is found to be the widest for ST 2 and ST 2RF water (this coincides with the wide hysteresis loop obtained for the ST 2RF model by quick isothermal compression/decompression [20]). The density interval of the two lower-density transitions in the ST 2 model practically coincides with the density range of the

first transition in the ST 2RF model. So, 3 supercooled phases (phases I, III and IV) are found for the ST 2RF model. Two liquid-liquid phase transitions and 3 supercooled phases (phases I and, presumably, phases II and III) we have found for TIP 4P, TIP 5P and SPCE water. The density range of the liquid-liquid transitions in each of these models is much narrower than in the ST 2 and ST 2RF models. The latter observation corroborates the

narrow hysteresis loop obtained for the TIP 4P model by quick isothermal compression/decompression [20].

The density of LDA (the lowest-density amorphous water phase observed experimentally) is about  $0.94 \text{ g cm}^{-3}$  at zero pressure and  $T = 77 \text{ K}$  [1]. At the same conditions, the density of HDA was reported from  $1.14\text{--}1.15 \text{ g cm}^{-3}$  in Ref.[61] to  $1.17\text{--}1.19 \text{ g cm}^{-3}$  in Ref.[1]), while the density of VHDA is about  $1.25\text{--}1.26 \text{ g cm}^{-3}$  [61]. Comparing with the densities of our isotherms at the same pressure we can attribute LDA to the lowest density phase (phase I) of the first liquid-liquid phase transition of all studied water models. HDA likely corresponds to phase III in all studied models, whereas VHDA could be attributed to phase IV, which is observed in ST 2 and ST 2RF water only.

Phase II, which is observed for all studied water models, except the ST 2RF model, usually corresponds to liquid water in equilibrium with the vapor (see the diamonds in Figs.12,17,19 and 20): in the whole studied temperature range of the TIP 4P and SPCE water models, above the triple point for the ST 2 model and below the triple point for the TIP 5P model. The density of phase II in the supercooled region of the ST 2, SPCE and TIP 5P models is about  $1.00\text{--}1.04 \text{ g cm}^{-3}$  and varies slightly with the temperature. For the TIP 4P water model phase II achieves the density  $1.14 \text{ g cm}^{-3}$  with decreasing temperature at zero pressure. The search of such a phase in real supercooled water seems to be a challenge for the experimental studies. There has been a single experimental observation of amorphous water (hyperquenched water) with the density  $1.04 \text{ g cm}^{-3}$ , reported in Ref.[62].

Experimentally, transitions between various amorphous ices can be studied directly at temperatures below  $T = 150 \text{ K}$ , i.e. below the temperature of the spontaneous crystallization of the amorphous water. At these temperatures the phase transition between HDA and LDA occurs at a pressure of  $P = 2 \text{ kbar}$  [55, 56, 65], which slightly increases upon cooling [65]. Measurements of the low-temperature melting curves of crystalline ices [66] provide an extension of the HDA/LDA transition line up to at least  $230 \text{ K}$  and down to pressures below  $+0.5 \text{ kbar}$ . The densities of the coexisting phases at the HDA/LDA phase transition is about  $0.94$  and  $1.20 \text{ g cm}^{-3}$  at  $T = 130 \text{ K}$  [65] and they do not change essentially upon cooling to  $T = 110 \text{ K}$  [55, 56]. Experimental data points for the water isotherm  $T = 110 \text{ K}$  [55, 56], are compared with the simulated  $T = 150 \text{ K}$  isotherm of TIP 4P water in Fig.17. The experimental hysteresis loop approximately covers the density interval, which corresponds to the two liquid-liquid transitions of the TIP 4P, TIP 5P and SPCE water models. This confirms our assignment of phase I to LDA and phase III to HDA. A comparison of the experimental and simulated data, shown in Fig.17 (lower panel) may also be used as an indication for the existence of phase II in real water. The location of the phase transitions of the TIP 4P model in the pressure-density plane is closer to the experiment, than of TIP 5P and

SPCE models. This conclusion is in line with the results of the computer simulations [67, 68], which show ability of the TIP 4P model to describe correctly the phase diagram of crystalline ices, unlike the SPCE and TIP 5P models. Note finally, that the ST 2 water model likely underestimates the densities of HDA and VHDA due to its overestimated tetrahedral structure.

Other common (universal) features of the phase behavior can be noticed. In particular, the second transition in all studied models (except the specific case of the ST 2RF model) seems to be rather universal. It is always located at positive pressures and its coexistence pressure increases with decreasing temperature. The proximity of the critical point of this transition to the liquid density maximum and to the consecutive density minimum allows to attribute the existence of these features to the influence of the second liquid-liquid phase transition. Indeed, above  $T_{\max}$  the influence of the liquid-vapor critical point on the density of the liquid branch is dominant and the temperature derivative of its density is negative, i.e. it shows normal behavior. Below  $T_{\max}$  the derivative  $(\partial/\partial T)_P$  is positive and the liquid branch can be considered as a supercritical isobar ( $P = 0$ ) of the second liquid-liquid phase transition. With further decreasing temperature, the zero pressure isobar turns to the "normal" behavior with  $(\partial/\partial T)_P < 0$  after the density minimum. This "normal" behavior of the isobar ( $P = 0$ ) in deeply supercooled region can be attributed to the tilt, i.e. the shift of the two-phase region of the second liquid-liquid phase transition toward higher densities with decreasing temperature (Fig.18) rather than to the influence of the distant liquid-vapor critical point. So, the liquid density minimum and its consecutive maximum appear to be the result of a crossover between the three regimes, described above. Note, that the critical temperature of the second liquid-liquid phase transition in all studied models appears above (or close to) the glass transition temperature.

The first liquid-liquid phase transition is much more sensitive to the choice of the water model and its implementation. This transition is located completely at positive pressures only for the ST 2RF water model, which does not provide a realistic water density at ambient pressures. It is located completely at negative pressures (TIP 4P and SPCE models), or it meets the liquid-vapor coexistence curve in a triple point (ST 2 and TIP 5P models). The critical point of this transition is located at slightly negative pressures for the ST 2, TIP 4P and SPCE models and at slightly positive pressure in the case of the TIP 5P model. Only for the ST 2 and TIP 4P models the critical point of the first liquid-liquid phase transition is above the estimated zero pressure glass transition temperature.

The line of the first liquid-liquid phase transition in the  $P$ - $T$  plane is characterized by an essentially negative slope for the ST 2 model and an essentially positive slope for the TIP 5P model, whereas it could not be determined for the TIP 4P and SPCE models. The presence

of a triple point, where the vapor coexists with two liquid phases, means, that the liquid branch of the liquid-vapor coexistence curve crosses the liquid-liquid spinodal at some temperature below the triple point temperature. Such crossing can explain the apparent singular behavior of some thermodynamic properties, which in real liquid water is observed at 228 K [69], i.e. 49 below the temperature of the density maximum. This scenario is very close to that observed for the ST2 model, where the triple point is located about 35 below  $T_{\max}$  and the liquid-liquid spinodal crosses the liquid-vapor coexistence curve at about 40 below  $T_{\max}$  [10]. The triple point for the TIP5P model is found about 100–125 below  $T_{\max}$  and therefore the liquid-liquid spinodal should cross the liquid-vapor coexistence curve far away from  $T_{\max}$ .

The magnitude of the increase of the heat capacity of liquid water with decreasing temperature, observed in all studied water models, seems to be highly sensitive to the location of the first liquid-liquid phase transition. In the TIP4P and SPC/E water models, which do not show a triple point, there is only weak gradual increase of  $C_p$  upon cooling. In TIP5P the absolute values of the heat capacity essentially exceed the experimental values in a wide temperature range. The strong increase of  $C_p$  upon cooling is interrupted by a glass transition and therefore the expected singularity below the triple point could not be observed. A singular-like behavior of  $C_p$  is observed for the ST2 water model when crossing the triple point.

The structure of liquid water in various thermodynamic states can be studied by the analysis of clustering and percolation [70]. In particular, the apparent singular behavior of some properties of liquid water in the supercooled region was attributed to the percolation of "four-bonded" water molecules [71]. This idea can be incorporated naturally in the observed phase behavior of supercooled water. Indeed, the percolation line of physical clusters of one of the constituting components should coincide with the spinodal of the phase transition, cross the coexistence curve in the critical point and extend into the one phase region [72, 73]. Thus, crossing the spinodal of a phase transition is equivalent to crossing a percolation line. The analysis of water clustering allowed localization of the percolation line in aqueous solutions with respect to the liquid-liquid phase transition [74]. We have applied this method also to identify the molecular species with different local order, which may be responsible for the liquid-liquid phase transitions in supercooled ST2 water [10, 75]. The first, lowest-density liquid-liquid transition is caused by separation of perfectly coordinated tetrahedral water molecules. With decreasing temperature along the liquid-vapor coexistence curve, the spinodal of the first liquid-liquid phase transition is crossed, which is a percolation line of the perfectly coordinated tetrahedral water molecules (Fig. 4 in Ref. [10]).

Based on our simulations of the phase diagram of various water models in the supercooled region, we can speculate about the possible location of liquid-liquid phase

transitions in real water. We may expect, that there are at least two liquid-liquid phase transitions in real water, which effect the properties of liquid water at ambient conditions. One transition should be located at positive pressures with its critical point close to the density maximum of liquid water. This transition seems to be responsible for the anomalous behavior of the liquid water density. Another transition should meet the liquid-vapor transition and the spinodal of this transition could be the origin of the experimentally observed thermodynamic singularities of liquid water at 228 K [69].

Finally, we would like to mention some perspectives for further studies of the phase behavior of liquids. The existence of various liquid phases of a one-component isotropic uid presumably is related to different kinds of short and intermediate range order in the liquids. Indeed, in water the liquid phase with the lowest density consists of perfectly tetrahedrally coordinated water molecules, whereas the liquid phase with the highest density consists mainly of water molecules with isotropic closely packed Lennard-Jones-like local order [10]. The main structural features of the other water phase(s) remain unclear and deserve further studies. It seems to be reasonable to analyze the structure of these phases, taking into account the various kinds of local ordering in crystalline ices.

In accord with the liquid-vapor phase transition, the uid density is usually considered as the order parameter of the liquid-liquid phase transition of a one-component uid. On the other hand, the concentration is the order parameter of liquid-liquid phase transitions in mixtures. In the case of a one-component uid, the concentration of molecules, showing some definite kind of local order, seems to be reasonable to consider as an order parameter of the liquid-liquid phase transition. Such an approach is reminiscent of the well-known two- and multi-states water models (see, for example Ref. [76]), originating from the idea of W. C. Roentgen from 1892 [77]. Note, that the mutual transformations between different kinds of local ordering in one-component uid violates the conservation of the concentrations of species. So, finding a more appropriate order parameters of the liquid-liquid phase transition in a one-component uid is an actual problem of the physics of liquids. Moreover, the universality class of this transition is not necessarily the universality class of the Ising model, as in the case of binary mixtures. For example, the possibility to change the local order continuously introduces unavoidable disorder, which could vary with thermodynamic conditions. This means, that the critical behavior of such a system could belong to the universality class of random field Ising models. We can not exclude, that the enhancement of disorder with increasing temperature could lead to a rounding of the phase transition and the disappearance of a true critical point. In this case the two coexisting liquid phases are not infinite and the two-phase state appears as a domain structure.

## Acknowledgments

We thank Deutsche Forschungsgemeinschaft, Forschergruppe 436, for financial support.

---

[1] O Mishima, L D C牢vert, and E W halley, *Nature* 314, 76 (1985).

[2] O Mishima and H. Stanley, *J. Chem. Phys.* 392, 164 (1998).

[3] O Mishima and Y Suzuki, *Nature* 419, 599 (2002).

[4] S Klotz, T. Strassle, R. J. Nelson, J. S. Loveday, G. Hamel, G. Rousse, B. Cann, J. C. Chervin, and A. M. Saitta, *Phys. Rev. Lett.* 94, 025506 (2005).

[5] P. H. Poole, F. Sciortino, U. Esmann, and H. E. Stanley, *Nature* 360, 324 (1992).

[6] P. H. Poole, F. Sciortino, U. Esmann, and H. E. Stanley, *Phys. Rev. E* 48, 3799 (1993).

[7] S. Harrington, R. Zhang, P. H. Poole, F. Sciortino, and H. E. Stanley, *Phys. Rev. Lett.* 78, 2409 (1997).

[8] M. Yamada, S. M. ossa, H. E. Stanley, and F. Sciortino, *Phys. Rev. Lett.* 88, 195701 (2002).

[9] M. Yamada, H. E. Stanley, and F. Sciortino, *Phys. Rev. E* 67, 010202 (2003).

[10] I. Brovchenko, A. Geiger, and A. Oleinikova, *J. Chem. Phys.* 118, 9473 (2003).

[11] I. Brovchenko, A. Geiger, and A. Oleinikova, *Proceedings of the 14th ICPS*, Kyoto (2004).

[12] P. Jedlovszky and R. Vallauri, *J. Chem. Phys.* 122, 081101 (2005).

[13] P. G. Debenedetti, *J. Phys.: Condens. Matter* 15, R1669 (2003).

[14] C. A. Angell, *Ann. Rev. Phys. Chem.* 55, 559 (2004).

[15] H. E. Stanley, S. V. Buldyrev, G. Franzese, N. G. Iovambattista, and F. W. Starr, *Phil. Trans. R. Soc. A* 363, 509 (2005).

[16] A. V. Voronel, *JETP Letters (Russ.)* 14, 174 (1971).

[17] M. A. Anisimov, A. V. Voronel, N. S. Zaugolnikova, and G. I. Ovodov, *JETP Letters (Russ.)* 15, 317 (1972).

[18] C. A. Angell, M. Oguni, and W. J. Sichina, *J. Phys. Chem.* 86, 998 (1982).

[19] L. J. MacDowell, P. V. Imai, M. Mueller, and K. Binder, *J. Chem. Phys.* 120, 5293 (2004).

[20] P. H. Poole, U. Esmann, F. Sciortino, and H. E. Stanley, *Phys. Rev. E* 48, 4605 (1993).

[21] F. Sciortino, P. H. Poole, U. Esmann, and H. E. Stanley, *Phys. Rev. E* 55, 727 (1997).

[22] S. Harrington, R. Zhang, P. H. Poole, F. Sciortino, and H. E. Stanley, *Phys. Rev. Lett.* 78, 2409 (1997).

[23] J.-P. Hansen and L. Verlett, *Phys. Rev.* 184, 151 (1969).

[24] H. Tanaka, *J. Chem. Phys.* 105, 5099 (1996).

[25] D. Paschek and A. Geiger, *J. Phys. Chem.* 103, 4139 (1999).

[26] D. S. Corti and P. G. Debenedetti, *Chem. Eng. Sci.* 49, 2717 (1994).

[27] W. Wagner and A. Pruss, *J. Phys. Chem. Ref. Data* 31, 387 (2002).

[28] B. V. Zheleznyi, *Russ. J. Phys. Chem.* 43, 1311 (1969).

[29] F. H. Stillinger and A. Rahman, *J. Chem. Phys.* 105, 5099 (1994).

[30] W. L. Jorgensen, J. C. Chandrasekhar, J. D. Madura, R. W. Impey, and M. L. Klein, *J. Chem. Phys.* 77, 926 (1982).

[31] M. W. Mahoney and W. L. Jorgensen, *J. Chem. Phys.* 112, 8910 (2000).

[32] H. J. C. Berendsen, J. R. Grigera, and T. P. Straatsma, *J. Phys. Chem.* 91, 6269 (1987).

[33] A. Z. Panagiotopoulos, *Mol. Phys.* 61, 813 (1987).

[34] I. Brovchenko, A. Geiger, and A. Oleinikova, *J. Chem. Phys.* 120, 1958 (2004).

[35] M. Lisal, J. K. Olaf, and I. Nezbeda, *J. Chem. Phys.* 117, 8892 (2002).

[36] S. Yoo and X. C. Zeng, *J. Chem. Phys.* 117, 9518 (2002).

[37] H. Tanaka, *J. Chem. Phys.* 113, 11202 (2000).

[38] W. L. Jorgensen and C. Jenson, *J. Comp. Chem.* 19, 1179 (1998).

[39] F. Saija, A. M. Saitta, and P. V. G. Iaquinta, *J. Chem. Phys.* 119, 3587 (2003).

[40] Y. Guissani and B. Guillot, *J. Chem. Phys.* 98, 8221 (1993).

[41] G. C. Boulougouris, I. G. Economou, and D. N. Theodorou, *J. Phys. Chem. B* 102, 1029 (1998).

[42] J. Vorholz, V. J. Harisimadis, B. Rumpp, A. Z. Panagiotopoulos, and G. M. Maurer, *Fluid Phase Equilibria* 170, 203 (2000).

[43] P. H. Poole, F. Sciortino, T. G. Grandjean, H. E. Stanley, and C. A. Angell, *Phys. Rev. Lett.* 73, 1632 (1994).

[44] L. A. Baez and P. Clancy, *J. Chem. Phys.* 101, 9837 (1994).

[45] L. A. Baez and P. Clancy, *J. Chem. Phys.* 103, 9744 (1995).

[46] S. Harrington, P. H. Poole, F. Sciortino, and H. E. Stanley, *J. Chem. Phys.* 107, 7443 (1997).

[47] F. W. Starr, M. C. Bellissent-Funel, and H. E. Stanley, *Phys. Rev. E* 60, 1084 (1999).

[48] T. Bryk and A. D. J. Haymet, *Mol. Simul.* 30, 131 (2004).

[49] S. W. Rick, *J. Chem. Phys.* 120, 6085 (2004).

[50] H. W. Horn, W. C. Swope, J. W. Pitera, J. D. Madura, T. J. Dick, G. L. Hura, and T. Head-Gordon, *J. Chem. Phys.* 120, 9665 (2004).

[51] I. Brovchenko, A. Geiger, and A. Oleinikova, *Phys. Chem. Chem. Phys.* 3, 1567 (2001).

[52] I. Brovchenko, A. Geiger, and A. Oleinikova, *New Kinds of Phase Transitions: Transformations in Disordered Substances*, V. V. Brazhkin, S. V. Buldyrev, V. N. Rhyzhov and H. E. Stanley (eds) *Proc. NATO Advanced Research Workshop*, Volga River, Kluver, Dordrecht) p. 367 (2002).

[53] B. Guillot and Y. Guissani, *J. Chem. Phys.* 119, 11740 (2003).

[54] C. A. Tulk, C. J. Bemore, J. J. Rodriguez, D. D. Kiang, J. Neuefeind, B. Tomberli, and P. A. Egelsta, *Science* 297, 1320 (2002).

[55] O. V. Stalgorova, E. L. Gromnitskaya, V. V. Brazhkin, and A. G. Lyapin, *JETP Letters (Russ.)* 69, 694 (1999).

[56] E. L. Gromnitskaya, O. V. Stalgorova, V. V. Brazhkin, and

A G Lyapin, *Phys. Rev. B* 64, 094205 (2001).

[57] A Scala, F W Starr, E. Nave, H E Stanley, and F Sciortino, *Phys. Rev. E* 62, 8016 (2000).

[58] H Tanaka, *Phys. Rev. E* 62, 6968 (2000).

[59] V V Brazhkin, R N Voloshin, A G Lyapin, and S V Popova, *Physics-U spekhi* 42, 941 (1999).

[60] V F Petrenko and R W Whithworth, *Physics of Ice* (Oxford University Press, Oxford) (1999).

[61] T Loerting, C Salzmann, I Kohl, E Mayer, and A Hallbrucker, *Phys. Chem. Chem. Phys.* 3, 5355 (2001).

[62] J. W. E. Brower, D J Schedler, and L K Bigelow, *J. Phys. Chem. B* 106, 4565 (2002).

[63] S V Buldyrev and H E Stanley, *Physica A* 330, 124 (2003).

[64] T M Truskett, P G Debenedetti, and S Torquato, *J. Chem. Phys.* 114, 2401 (2001).

[65] O Mishima, *J. Chem. Phys.* 100, 5910 (1994).

[66] O Mishima, *Phys. Rev. Lett.* 85, 335 (2000).

[67] E Sanz, C Vega, J L F Abascal, and L G MacDowell, *J. Chem. Phys.* 121, 1165 (2004).

[68] C Vega, E Sanz, and J L F Abascal, *J. Chem. Phys.* 122, 114507 (2005).

[69] R J Speedy and C A Angell, *J. Chem. Phys.* 65, 851 (1976).

[70] A Geiger, F H Stillinger, and A Rahman, *J. Chem. Phys.* 70, 4185 (1979).

[71] H. Stanley and J. Teixeira, *J. Chem. Phys.* 73, 3404 (1980).

[72] A Coniglio and W Klein, *J. Phys. A* 13, 25 (1967).

[73] W Klein, *J. Phys. A* 47, 1569 (1981).

[74] A Oleinikova, I Brovchenko, A Geiger, and B Guillot, *J. Chem. Phys.* 117, 3296 (2002).

[75] I Brovchenko, A Geiger, and A Oleinikova, to be published (2005).

[76] G W Robinson, S-B. Zhu, S Singh, and M. Evans, Water in Biology, Chemistry and Physics: Experimental Overview and Computational Methodologies, World Scientific, Singapore (1996).

[77] W C Roentgen, *Annalen der Physik und Chemie* 45, 91 (1892).